ELSEVIER

Earth and Planetary Science Letters 202 (2002) 379–386

EPSL

www.elsevier.com/locate/epsl

Cretaceous length of day perturbation by mantle avalanche

Philippe Machetel *, Emilie Thomassot

ISTEEM, Laboratoire de Tectonophysique, UMR 5568 CNRS/UM2, Place Eugène Bataillon, 34095 Montpellier Cedex 5, France

Received 25 March 2002; received in revised form 11 June 2002; accepted 14 June 2002

Abstract

These last 10 years, numerical models of mantle convection have emphasized the role of the 670 km endothermic phase change in generating avalanches that trigger catastrophic mass transfers between upper and lower mantle. On the other hand, scientists have emphasized the concomitance of large-scale worldwide geophysical and tectonic events, which could find their deep thermal roots in the huge mass transfers induced by the avalanches. In particular, the paleontological records show two periods of length of day (l.o.d.) shortening between 420 and 360, and 200 and 80 Myr BP. This last event is synchronous with a strong true polar wander and a global warming of the upper mantle. In order to study the potential effects of the avalanche on the main component of the Earth's rotation, the Liouville equation has been solved and the l.o.d. evolution has been calculated from the perturbations of the inertia tensor. The results show that the inertia tensor of the Earth's is mainly sensitive to the global transfers through the 670 km discontinuity. The l.o.d. perturbations will be synchronous with the global thermal effects of the avalanche. These theoretical results allow proposing a self-consistent physical mechanism to explain periods of the Earth's rotation acceleration. Within this context, the l.o.d. shortening during the Cenozoic and Cretaceous brings one more clue to the possible participation of a mantle avalanche in generating the concomitant large scale events which have occurred during this very particular period of the Earth's history.

Keywords: mantle; convection; avalanches; Earth; rotation; length of day

1. Context in theoretical mechanics of the fluid mantle

For approximately 10 years, numerical models of convection which include the main mantle phase changes have depicted intermittently layered convection in the mantle, due to the endothermic character of the 670 km spinel−perovskite+magnesiowustite phase change. This regime, which is characterized by periods of quiet partial layering wedged between catastrophic overturns (the avalanches), has been found by numerous authors with independent numerical codes based on 2-D spherical geometry [1–3], 3-D spherical geometry [4–6], and 2-D and 3-D Cartesian geometries [7,8]. The convergence of these numerical results does not mean that the scientific question about the global structure of mantle convection is definitively resolved, but that the fluid dynamical pattern with partial layering and intermittent avalanches is very robust. Finally, this pattern has been found with various internal heating rates

* Corresponding author. Tel.: +33-4-67-14-45-93; Fax: +33-4-67-14-47-85.
E-mail address: machetel@dstu.univ-montp2.fr (P. Machetel).

0012-821X/02/$ – see front matter
PII: S0012-821X(02)00785-9

(from 0 to chondritic), with temperature and pressure dependent viscosities, and with various viscosity stratifications [3,9].

2. The Earth's history context

Attempts have been made to extend these theoretical fluid mechanical results to the problem of a secularly cooling Earth. The early Earth's history is characterized by huge heat accumulation from accretion and higher radioactivity rates that necessarily induced higher mantle temperatures and reduced mantle viscosity. Therefore, the Rayleigh number of this early mantle was much higher than the present one. According to the numerical simulations, which show that the more the Rayleigh number is raised, the more the structure of the convection tends to be layered, the mantle probably had two layers at that time [10–12]. The present scientific debate about the mantle structure is balancing between a one- and a partly layered mantle that allows closer simulation of the geoid by kinematic models [13]. A monotonic, decreasing Rayleigh number evolution, since an early-layered structure to a partially layered or a one-layered present structure for mantle, implies that an avalanche-like regime was crossed during the past or is presently active.

Recently, scientists have emphasized the concomitance of large scale, worldwide geophysical and tectonic events, such as the stopping of the geodynamo reversal [14–16] (Fig. 1, row a); the major break-up of continents [17,18]; the global oceanic ridge accelerations (Fig. 1, curve f) and their possible consequences in terms of CO_2 atmospheric content) [19] (Fig. 1, curve j), sea level [20] (Fig. 1, curve i), oil, gas and coal deposits [21,22] (Fig. 1, curves c–e); and the superplume activity [23] (Fig. 1, row b and curve g). These events find their deep thermal origin in the mantle or directly depend on thermal mantle anomalies. This is particularly true for the geodynamo reversals, which are very sensitive to the heat flux configuration at the core–mantle boundary (CMB) [24]. According to their common thermal links, their mantle-wide spatial extents and their several tens of million year durations, these phenomena

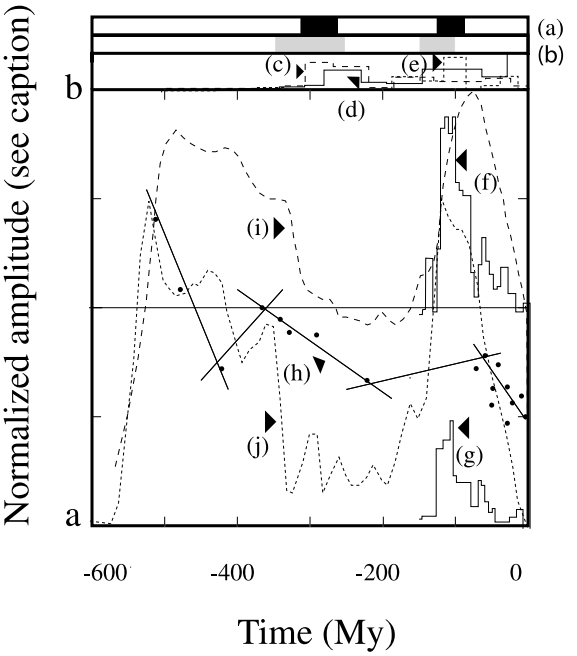

Fig. 1. Compilation of geophysical observations for the Phanerozoic eon. Vertical axis is linear and normalized for each curve as follows. (a) Superchron periods; (b) age of basaltic magmatism in accretionary complexes and oceanic plateaus; (c–e) estimations of world fossil fuel resources for coal, gas and oil; (f) non-cumulative histogram of the world oceanic crust production ($a=0$, $b=35\times10^6$ km^3/Myr); (g) same as (f) for oceanic plateaus (same scaling); (h) number of synodic days by synodic month ($a=28$ days/month, $b=33$); (i) Phanerozoic first order eustatic sea level; (j) rate of volcanic and metamorphic degassing of CO_2 (see text for detailed references).

are necessarily coupled through the mass, energy and momentum equations governing mantle convection. Mantle avalanches have similar spatial scale and duration. They involve enough mass transfers to be considered the possible driving force of such mechanisms. The purpose of this work is to monitor the effects of such events on the main component of the Earth's rotation. Indeed, studies of seasonal fluctuations of coral growth and their daily growth increments, combined with the tidally controlled growth patterns exhibited by fossil mollusks, made it possible to retrieve the synodic and the annual number of days throughout the Phanerozoic eon (see e.g. the description given by Lambeck [25]). Curve h of Fig. 1 is redrawn from fig. 2 of the compilation

of the evolution of the number of synodic days by synodic month proposed by Creer [26]. The points exhibit five trends that make it possible to decipher periods of Earth's rotation slowing and periods of Earth's rotation acceleration (between 420 and 360 Myr and between 220 and 80 Myr). These trends are also verified for the number of days by year (in fig. 3 of Creer's paper [26]).

3. Theoretical aspects

In order to study the first order effect of a mantle avalanche on the main component of the Earth's rotation, the results of a new set of convection computations have been focused on the thermal evolution of the different parts of the mantle and on the mass transfers. The temperature and motion equations of spherical, axisymmetrical compressible convection have been solved with an exothermic phase change at 400 km, an endothermic phase change at 670 km, a temperature and pressure dependent viscosity and a viscosity jump of 30 between the upper and lower mantle. Full descriptions of the numerical methods and of the physical and geophysical hypothesis are given in detail in a recent work by Brunet and Machetel [3], which was mainly concerned with the global geodynamic consequences of the avalanches. The avalanches occur according to a chaotic process, which illustrates the compromise between a global thermal state of the mantle and its local recent history. The unrolling of the sequence reveals firstly a partial layering of convection (low mixing rate between the upper and the lower mantle) that induces an insulation of the lower mantle. An increase of the lower mantle temperature results, which induces a decrease of its viscosity. Simultaneously, efficient convection cools the upper mantle and increases its viscosity. This process increases the difference in temperature on both sides of the 670 km discontinuity. When a certain threshold is exceeded, a destabilization of the boundary layer occurs that results in a brutal and massive injection of cold upper mantle materials into the lower mantle (period of increasing mixing: 500–750 Myr, Fig. 2). The upper mantle is attracted in a broad volume around the epicenter whereas rising currents originating from the lower mantle cross the 670 km discontinuity in several places to compensate the avalanche. A few tens of million years later, the cold sinking material spreads on the core by sweeping the (softer) CMB boundary layer and generating buoyant plumes. As a consequence of cold upper mantle material injection, the lower mantle is cooled by about 20 K while the return flows induce a 50 K increase of the mean upper mantle temperature (Fig. 2). Both effects tend to reduce the temperature difference through the 670 km discontinuity whose stability is restored (return to low mixing rate).

Following Munk and MacDonald [27], the Eulerian equations of motions in a coordinate system x_i ($i=1,2,3$), rotating with angular velocity ω_i relative to coordinate X_i fixed in space and coinciding with x_i for the moment are:

$$L_i = \frac{\mathrm{d}H_i}{\mathrm{d}t} + \varepsilon_{ijk}\omega_j H_k \tag{1}$$

where L_i are the components of external torque, H_i those of angular momentum and ε_{ijk} is the alternating tensor. It is convenient to separate this general equation into two parts with:

$$H_i = C_{ij}(t)\omega_j + h_i(t) \tag{2}$$

where

$$C_{ij} = \int_V \rho(x_k x_k \delta_{ij} - x_i x_j)\mathrm{d}V \tag{3}$$

is the tensor of inertia and δ_{ij} is the Kronecker symbol. $h_i(t)$ designates a relative angular momentum, which will be zero in the case of a solid rotating body. As the purpose of this study is to monitor the rotation perturbations induced by the mass redistribution during mantle avalanches, we will consider the Earth as an isolated body in space by setting $L_i = 0$. Finally, we will have to solve the Liouville equation:

$$\frac{\mathrm{d}}{\mathrm{d}t}(C_{ij}\omega_j) + \varepsilon_{ijk}\omega_j C_{kl}\omega_l = 0 \tag{4}$$

In the following, only the third component of Eq. 4 will be used, as it is pertinent for the length

of day (l.o.d.) studies [27]. With the reasonable assumption that the inertia tensor and the angular velocity perturbation can be written as small perturbations of the main components: $C_{11} = A+c_{11}$, $C_{22} = A+c_{22}$, $C_{33} = C+c_{33}$; $C_{ij} = c_{ij}$ for $i \neq j$; $\omega_1 = \Omega m_1$, $\omega_2 = \Omega m_2$ and $\omega_3 = \Omega(1+m_3)$ (c_{ij}/C and m_i being small quantities, whose square and products can be neglected), then the third component of the Liouville equation reduces to:

$$\frac{dm_3}{dt} = -\frac{1}{C}\frac{dc_{33}}{dt} \quad (5)$$

where C is the Earth's equatorial moment of inertia, $C = 8.068 \times 10^{37}$ kg m^2. The knowledge of the inertia tensor evolution with time will allow the computation of the Earth's rotation velocity and therefore the l.o.d.

4. Evolution of the mantle temperature and mass

To follow more accurately the mantle mass transfers, the global mantle (GM) has been divided into three parts: (1) the upper mantle UM (from the lithospheric plate to the 400 km discontinuity), (2) the transition zone TZ (zone between the 400 km and the 670 km discontinuities), and (3) the lower mantle LM (from the 670 km discontinuity to the CMB). The positions of the boundaries of these layers and therefore their masses and volumes vary during the avalanche since they depend on the temperature and on the pressure through the Clapeyron slopes of the phase changes.

A quiet period of layering, with UM and TZ cooling and LM heating, can be recognized from 250 to 500 Myr, when the flux of matter through the 670 km discontinuity is low. The rate falls to 250×10^6 km^3/Myr, that is 5–10 times lower than the typical values reached during the paroxysmal phases of the avalanches. As expected from the replacement of cold upper mantle material (UM+TZ) by hot LM rising currents, the UM and TZ temperatures increase after the start of strong flux periods (Fig. 2). The delay of UM increase of temperature corresponds to the time necessary for the return flow to cross TZ. On the other hand, the avalanche cools the LM during the high flux phase.

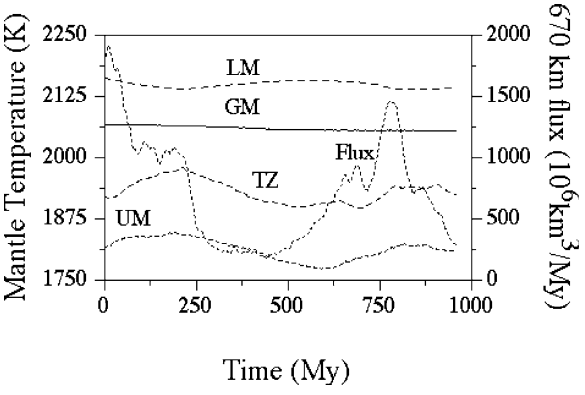

Fig. 2. Evolutions of the mean temperatures for the global mantle (GM), the upper mantle (UM), the transition zone (TZ), and the lower mantle (LM). Flux is the flux of matter integrated through the 670 km discontinuity.

The evolution of the inertia tensor of the mantle will depend on the amplitude of the density anomalies and on their distance to the axis. Indeed, a local variation of temperature will change the density by thermal expansion, but also by phase changing. The third aspect, the position of the density variations, is directly taken into account by the computation process. With finite difference methods, the positions of the nodes of the computation grid do not vary with time in spite of thermal dilatations (or contractions) that induce spurious total mantle mass variations (Fig. 3). This is an indirect consequence of the anelastic-Boussinesq approximation, which stipulates that, for fluid motion, the density variations are only important for the gravity term of the Navier–Stokes equation. This approximation is justified for the calculation of the thermodynamic state of the fluid but needs to be revisited in order to compute accurate mantle masses and inertia tensor evolution. To address this question, the volume of each grid cell has been corrected for its dilatation (or contraction) with respect to the reference density. Then, the integration of density over the mantle volume remains constant and equal to the total mantle mass in spite of free local variations. The second step of this correction has been to re-compute the radial position of each grid point by assuming that the volume contrac-

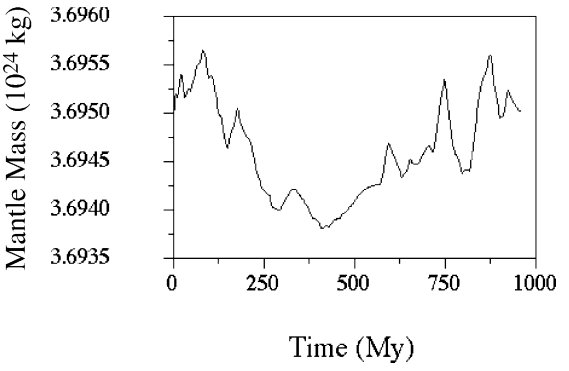

Fig. 3. Apparent evolution of the total mass of the mantle due to the fixed grid assumption of the numerical code.

tion (or dilatation) of each cell was supported by a radial deformation. Finally, the LM, TZ, and UM mass and the inertia tensor have been computed on a finite difference grid displaying 201 radial levels for 513 latitudinal points. This high resolution allows density anomalies of around 40 km lateral and radial extents that would correspond to a spectral decomposition up to harmonic 256.

Fig. 4 displays the mass evolution of the mantle parts and their inertia contribution through time. Finally, as a consequence of the radius-square dependence of the inertia tensor, the mantle part contributions to inertia follow closely but not exactly the evolution of the mass. During the quiet period (from 250 to 500 Myr), the cooling of UM and TZ raises the 400 km discontinuity. The simultaneous heating of lower mantle increases the amplitude of the thermal layer at the 670 km level but does not change the temperature at the boundary itself. The depth of the discontinuity remains the same and the LM mass and its contribution to the inertia tensor remain roughly constant. In summary, during the quiet periods, the TZ thickens at the expense of UM while LM remains approximately constant. The effects on the UM and TZ inertia compensate while the inertia of LM remains roughly constant.

When an avalanche occurs around 500 Myr, the bottom of the transition zone is immediately subjected to two opposite effects: a local deepening of the 670 km discontinuity around the avalanche epicenter due to the arrival of cold UM material and, distributed elsewhere along the return flows, local rising of the 670 km discontinuity by the hot return flows. These opposite contributions explain that the TZ mass and its inertia contribution remain roughly constant well after the starting of the avalanche (Fig. 4, middle). However, a few tens of million years later, as soon as the rising return flows reach the UM, the increase of temperature deepens the 400 km discontinuity that contributes to increase the mass of the UM. During this stage, the increase of the UM volume, going with the deepening of the TZ–LM boundary (global cooling of the lower mantle) corresponds, at almost constant TZ mass, to a global deepening of the TZ zone. Since the TZ density is higher than the UM one, this deepening induces a transfer of heavier masses toward the rotation axis and therefore a decrease of inertia.

The balance between the decrease of LM inertia

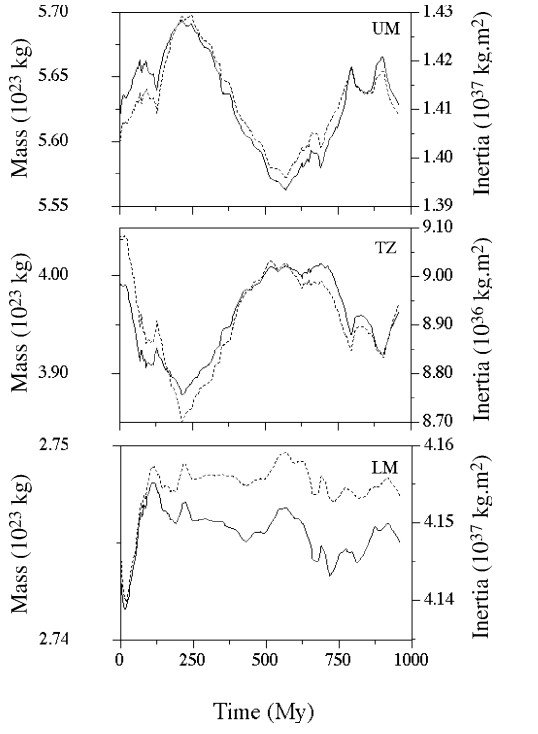

Fig. 4. Evolution of mass (solid curves) and of the C component of the inertia tensor (dashed curves) for the UM, the TZ and the LM.

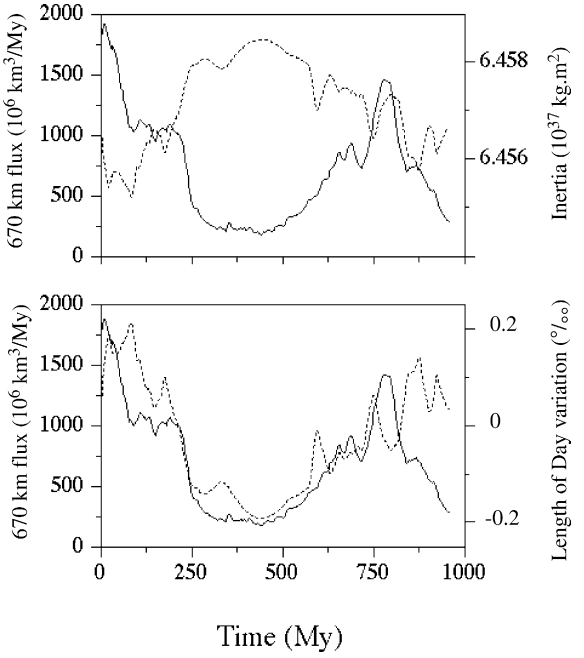

Fig. 5. Flux of matter through the 670 km discontinuity (top and bottom solid lines); evolution of the inertia tensor (top dashed line); calculation of the l.o.d. evolution (m_3/ω_3).

(due to its decreasing mass), the decrease of TZ inertia (due to its deepening) and the increase of UM inertia (due to its increasing mass) is given in Fig. 5 with the evolution of the daily rate of rotation (m_3/ω_3). The ω_3 variations follow with a slight delay the variations of flux through the 670 km boundary. The rotation remains almost constant during the quiet period (from 250 to 500 Myr), but increases as soon as the avalanche occurs.

In summary, these computations show that the inertia tensor of the Earth is not very sensitive to the cooling of UM and TZ by partial layering while it is sensitive to the mass transfers between UM and LM because they induce global thermal perturbations that tend to deepen the TZ. The l.o.d. perturbations will be synchronous with the global thermal effects due to the avalanche. During the quiet period of layering the main component of the Earth's rotation remains roughly constant while the rotation of the Earth accelerates with the deepening of the TZ when the avalanche occurs (Fig. 5).

5. Avalanche induced l.o.d. perturbations during the Cretaceous?

From global tectonic considerations [28], one can expect, as a working hypothesis, that an avalanche may have started around 190–180 Myr BP at the time of the convergence of the Thetys Ocean. A more serious indication for the occurrence of a mantle avalanche may be the starting of a new episode of true polar wander at 170 Myr [29,30] which could have been induced by major mantle mass redistribution [31]. The change of geodynamo reversal rate [15,32] and the beginning of the superplume activity in the Polynesian superswell region [23] are associated with the spreading of the avalanche onto the core and with the surface arrival of lower mantle return flows. From curve h of Fig. 1, a global trend for l.o.d. shortening can be evaluated between 200 and 80 Myr. Indeed, even though an unfortunate gap exists in the data set around this period, the global trends just before 200 Myr and just after 80 Myr are clearly a monotonic lengthening of the l.o.d., with a clear shortening between. This event is synchronous with a strong true polar wander event, which reaches a maximum value of 5°/Myr [29], and a global warming of the upper mantle [33]. This is also synchronous with LM contaminations of the Atlantic ridge from 160 to 120 Myr [34] and the Pacific ridge (151–130 Myr) [35]. Later, from 125 Myr to 85 Myr, the reversal of the geomagnetic field ceases for 40 Myr. Simultaneously, the superplume activity is strong, as attested by the oceanic plateau production and the global rate mid-oceanic ridge accretion is almost double of those of the late Cenozoic [36].

Our theoretical calculations show that an avalanche is able to significantly disturb the inertia tensor of the Earth because it results in a deep and global perturbation of the thermal field that induces a significant deepening of the transition zone. This effect is compatible with a long term variation of temperature during the quiet periods of partial layering since the opposite signs of the Clapeyron slopes at 400 km and 670 km allow the compensation of the mass and inertia effects of phase transitions between UM and TZ as long as the mass transfers between LM and UM+TZ

are low. We are presently developing a new 3-D numerical code in order to extend these results to a more general study of the effects of avalanches on Earth's rotation including the l.o.d. but also the polar wander. The confrontation with the Cenozoic–Cretaceous geophysical observations brings one more reason to suspect the occurrence of a mantle avalanche during the Cenozoic–Cretaceous periods. Indeed, the possibility of accelerating the rotation of the Earth was not considered seriously in the absence of a credible physical mechanism. Indeed, diminutions of friction related to sea level changes are only able to reduce the deceleration, but not to reverse the trend toward acceleration. Of course, these results ask the question of the reliability of paleontological data. Although we have to be aware of this, there is no a priori reason to question one point of curve h of Fig. 1 more than the other. It has also to be emphasized that our results add one more independent observation of a global change, concomitant with the other phenomena that have perturbed this very particular period of the Earth's history.

Acknowledgements

The authors thank P. Camps, M. Prévot, D. Rousseau and D. Mainprice for stimulating discussions; Eliane Nadal for her help in managing the computational sequence. This work is an INSU-Intérieur de la Terre program contribution. *[AC]*

References

[1] P. Machetel, P. Weber, Intermittent layered convection in a model mantle with an endothermic phase change at 670 km, Nature 350 (1991) 55–57.
[2] L.P. Solheim, W.R. Peltier, Avalanche effects in phase transition modulated thermal convection: a model of Earth's mantle, J. Geophys. Res. 99 (1994) 6997–7018.
[3] D. Brunet, P. Machetel, Large-scale tectonic features induced by mantle avalanches with phase, temperature, and pressure lateral variations of viscosity, J. Geophys. Res. 103 (1998) 4929–4945.
[4] P.J. Tackley, D.J. Stevenson, G.A. Glatzmaier, G. Schubert, Effects of an endothermic phase transition at 670 km depth in a spherical model of convection in the Earth's mantle, Nature 361 (1993) 699–704.
[5] P. Machetel, C. Thoraval, D. Brunet, Spectral and geophysical consequences of 3-D spherical mantle convection with an endothermic phase change at the 670 km discontinuity, Phys. Earth Planet. Inter. 88 (1995) 43–51.
[6] H.-P. Bunge, M.A. Richards, J.R. Baumgardner, A sensitivity study of three-dimensional spherical mantle convection at 108 Rayleigh number: effects of depth-dependent viscosity, heating mode, and an endothermic phase change, J. Geophys. Res. 102 (1997) 11991–12007.
[7] S.A. Weinstein, Catastrophic overturn of the Earth's mantle driven by multiple phase changes and internal heat generation, Geophys. Res. Lett. 20 (1993) 101–104.
[8] S. Honda, D.A. Yuen, S. Balachandar, D. Reuteler, Three-dimensional instabilities of mantle convection with multiple phase transitions, Science 259 (1993) 1308–1311.
[9] P. Machetel, Constraints on mantle structure from seismological and convection results, in: M.J.L. Le, D.E. Smylie, T. Herring (Eds.), Dynamics of Earth's Deep Interior and Earth Rotation, Geophysical Monograph 72, American Geophysical Union, Washington, DC, 1993, pp. 167–180.
[10] D.A. Yuen, U. Hansen, W. Zhao, A.P. Vincent, A.V. Malevsky, Hard turbulent thermal convection and thermal evolution of the mantle, J. Geophys. Res. 98 (1993) 5355–5373.
[11] V. Steinbach, D.A. Yuen, Effects of depth-dependent properties on the thermal anomalies produced in flush instabilities from phase transitions, Phys. Earth Planet. Inter. 86 (1994) 165–183.
[12] D.A. Yuen, S. Balachandar, V.C. Steinbach, S. Honda, D.M. Reuteler, J.J. Smedsmo, G.S. Lauer, Non-equilibrium effects of core-cooling and time dependent internal heating on mantle flush events, Nonlinear Process. Geophys. 2 (1995) 206–221.
[13] C. Thoraval, P. Machetel, A. Cazenave, Locally layered convection inferred from dynamic models of the Earth's mantle, Nature 375 (1995) 777–780.
[14] V. Courtillot, J. Besse, Magnetic field reversals, polar wander and core-mantle coupling, Science 237 (1987) 1140–1146.
[15] Y. Gallet, G. Hulot, Stationay and nonstationary behaviour within the geomagnetic polarity time scale, Geophys. Res. Lett. 24 (1997) 1875–1878.
[16] Y. Tatsumi, T. Kami, H. Ishizuka, S. Maruyama, Y. Nishimura, Activation of Pacific mantle plume during the Carboniferous: Evidence from accretionary complexes in Southwest Japan, Geology 28 (2000) 580–582.
[17] E.A. Eide, T.H. Torsvik, Paleozoic supercontinental assembly, mantle flushing, and genesis of the Kiaman Superchron, Earth Planet. Sci. Lett. 144 (1996) 389–402.
[18] V. Courtillot, C. Jaupart, I. Manighetti, P. Tapponnier, J. Besse, On causal links between flood basalts and continental breakup, Earth Planet. Sci. Lett. 166 (1999) 177–195.

[19] R.A. Berner, Atmospheric carbon dioxide levels over Phanerozoic time, Science 249 (1990) 1382–1386.
[20] S. Gaffin, Ridge volume dependence on seafloor generation rate and inversion using long term sealevel change, Am. J. Sci. 287 (1987) 596–611.
[21] R.L. Larson, Latest pulse of Earth: evidence for a mid-Cretaceous superplume, Geology 19 (1991) 547–550.
[22] R.L. Larson, Geological consequences of superplumes, Geology 19 (1991) 963–966.
[23] Y. Tatsumi, H. Shinjoe, H. Ishizuka, W.W. Sager, A. Klaus, Geochemical evidence for a mid-Cretaceous superplume, Geology 26 (1998) 151–154.
[24] G.A. Glatzmaier, R.S. Coe, L. Hongre, P.H. Roberts, The role of the Earth's mantle in controlling the frequency of geomagnetic reversals, Nature 401 (1999) 885–890.
[25] K. Lambeck, The Earth's Variable Rotation; Geophysical Causes and Consequences, Cambridge University Press, Cambridge, 1980, 449 pp.
[26] K.M. Creer, On a tentative correlation between changes in the geomagnetic polarity bias and reversal frequency and the Earth's rotation through phanerozoic time, in: G.D. Rosenberg, S.K. Runcorn (Eds.), Growth Rhythms and the History of the Earth's Rotation, John Wiley and Sons, London, 1974, pp. 293–317.
[27] W.H. Munk, G.J.F. MacDonald, The Rotation of the Earth, Cambridge University Press, 1960, 323 pp.
[28] G.M. Stampfli, Tethyan oceans, in: E. Bozkurt, J.A. Winchester, J.D.A. Piper (Eds.), Tectonics and Magmatism in Turkey and the Surrounding Area, Geological Society of London Special Publication 173 (2000) 1, 23.
[29] M. Prévot, E. Mattern, P. Camps, M. Daignières, Evidence for a 20° tilting of the Earth's rotation axis 110 million years ago, Earth Planet. Sci. Lett. 179 (2000) 517–528.
[30] J. Besse, V. Courtillot, Apparent and true polar wander and the geometry of the geomagnetic field in the last 200 million years, in press, 2002.
[31] M.A. Richards, H.-P. Bunge, Y. Ricard, J.R. Baumgardner, Polar wandering in mantle convection models, Geophys. Res. Lett. 26 (1999) 1777–1780.
[32] P.L. McFadden, R.T. Merril, Evolution of the geomagnetic reversal rate since 160 Ma: is the process continuous?, J. Geophys. Res. 105 (2000) 28455–28460.
[33] P. Machetel, E. Humler, High mantle temperature during Cretaceous, submitted, 2002.
[34] P.E. Janney, P.R. Castillo, Geochemistry of the oldest Atlantic oceanic crust suggests mantle plume involvement in the early history of the central Atlantic Ocean, Earth Planet. Sci. Lett. 192 (2001) 291–302.
[35] P.E. Janney, P.R. Castillo, Geochemistry of Mesozoic Pacific mid-ocean ridge basalt: constraints on melt generation and the evolution of the Pacific upper mantle, J. Geophys. Res. 102 (1997) 5207–5229.
[36] M.A. Richards, D.C. Engebretson, Large-scale mantle convection and the history of subduction, Nature 355 (1992) 437–440.